Bull Math Biol
DOI 10.1007/s11538-013-9852-3

Society for Mathematical Biology

ORIGINAL ARTICLE

Dynamics of Phytoplankton Communities Under Photoinhibition

Sze-Bi Hsu · Chiu-Ju Lin · Chih-Hao Hsieh ·
Kohei Yoshiyama

Received: 8 November 2012 / Accepted: 29 April 2013

Abstract We analyzed a model of phytoplankton competition for light in a well-mixed water column. The model, proposed by Gerla et al. (Oikos 120:519–527, 2011), assumed inhibition of photosynthesis at high irradiance (photoinhibition). We described the global behavior through mathematical analyses, providing a general solution to the multi-species competition for light with photoinhibition. We classified outcomes of 2- and 3-species competitions as examples, and evaluated feasibility of the theoretical predictions using empirical relationships between photosynthetic production and irradiance. Numerical simulations with published *p*–*I* curves indicate that photoinhibition may often lead to strong Allee effects and competitive facilitation among species. Hence, our results suggest that photoinhibition may play a major role in organizing phytoplankton communities.

Keywords Competition for light · Photoinhibition · Allee effect · Competitive facilitation · Alternative stable states

---

S.-B. Hsu (✉)
National Center for Theoretical Sciences, Hsinchu 300, Taiwan
e-mail: sbhsu@math.nthu.edu.tw

S.-B. Hsu · C.-J. Lin
Department of Mathematics, National Tsing-Hua University, Hsinchu 300, Taiwan

C.-J. Lin
e-mail: d9621806@oz.nthu.edu.tw

C.-H. Hsieh
Institute of Oceanography and Institute of Ecology and Evolutionary Biology, National Taiwan University, Taipei 10617, Taiwan
e-mail: chsieh@ntu.edu.tw

K. Yoshiyama
River Basin Research Center, Gifu University, Gifu 501-1193, Japan
e-mail: kyoshi@gifu-u.ac.jp

1 Introduction

Light is an essential resource for photosynthesis and the major source of energy for both terrestrial and aquatic ecosystems. Excess light, however, causes damage to the photosynthetic machinery, and thereby lessens photosynthetic production. This phenomenon, known as photoinhibition, is prevalent to all photosynthetic organisms from cyanobacteria to higher plants. The molecular mechanisms have been investigated intensively (Tyystjärvi 2008), and unimodal photosynthesis and irradiance (p–I) relationships of algal species were observed in laboratories (Henley 1993). The corresponding theoretical frameworks were proposed (Eilers and Peeters 1988; Zonneveld 1998; Han 2002; Muller 2010), which are in good agreement with measured p–I relationships. Field observations showed impacts of photoinhibition on ecosystem-level properties such as the magnitude and spatial variations of primary productivity in aquatic ecosystems (Alderkamp et al. 2010; Baastrup-Spohr and Staehr 2009; Basterretxea and Aristegui 2000; Bischof et al. 1998; Elser and Kimmel 1985; Oliver et al. 2003). However, influences of photoinhibition on ecological community structure are rarely investigated both empirically and theoretically.

One exception is Gerla et al. (2011), where they extended the classical light competition model of phytoplankton (Huisman and Weissing 1994; Weissing and Huisman 1994) by including the effect of photoinhibition (see also Huisman 1997). Their results suggested that phytoplankton population may exhibit a strong Allee effect and competitive facilitation. A strong Allee effect is a phenomenon that population goes extinct when the density is below a threshold, while it persists when the density is above the threshold. Competitive facilitation is a phenomenon that a species that cannot grow in monoculture can grow and take over the community under the presence of another species. Their theory and predictions, based on previous results of Huisman and Weissing (1994), Weissing and Huisman (1994) and graphical approach, indicated significance of photoinhibition in shaping phytoplankton community structure.

In this paper, we aim at analyzing the global dynamical behavior of a phytoplankton competition model with photoinhibition proposed by Gerla et al. (2011), and at evaluating feasibility of the theoretical predictions using empirical p–I curves compiled by Schwaderer et al. (2011). In doing so, we supplement the theory of Gerla et al. (2011), and shed light on the significance of photoinhibition in elucidating phytoplankton community structure in nature.

2 The Model and Main Results

Consider a model of n phytoplankton species competing for light in a well-mixed water column. The depth of the water column z ranges from 0 (the water surface) to $z_{\max}$ (the bottom of the water column). Let $x_i(t)$ be the population density of the ith species per unit surface area of water at time t. The governing equation for the ith species takes the form: (see Gerla et al. 2011; Weissing and Huisman

1994)

$$\frac{dx_i}{dt} = \left(\frac{1}{z_{\max}} \int_0^{z_{\max}} p_i\big(I(z,t)\big)\,dz - d_i\right)x_i, \quad i = 1, 2, \ldots, n. \tag{1}$$

The first term within the parentheses denotes the specific production rate averaged vertically in the water column, where $p_i(I)$ is the specific production rate as a function of light $I(z,t)$. The second term d_i denotes the specific loss rate.

According to Lambert–Beer's law, the light intensity at depth z and time t is expressed by

$$I(z,t) = I_{\mathrm{in}} \exp\left(-\sum_{j=1}^{n} k_j x_j(t) z \Big/ z_{\max} - K_{\mathrm{bg}} z\right), \tag{2}$$

where I_{in} is the incident light intensity at the top of the water column, k_j, the specific light attenuation coefficient of j-th species, and K_{bg}, the background light attenuation coefficient. Division by $z_{\max}$ in the first term within the parentheses converts the population density per unit surface area (x_j) to population density per unit volume ($x_j/z_{\max}$). Following Huisman and Weissing (1994), Weissing and Huisman (1994), we define I_{out} to be the light intensity at the bottom of the water column

$$I_{\mathrm{out}}(t) = I(z_{\max}, t) = I_{\mathrm{in}} \exp\left(-\sum_{j=1}^{n} k_j x_j(t) - K_{\mathrm{bg}} z_{\max}\right). \tag{3}$$

The specific production rate $p_i(I)$ decays when the light is too strong, known as photoinhibition (Schwaderer et al. 2011). General assumptions of such function are: $p_i(I) \geq 0$ and $dp/dI < \infty$ for $I > 0$, $p_i(0) = 0$, and

$$\begin{aligned} \frac{dp_i}{dI} &> 0 \quad \text{for } 0 \leq I < I_{\mathrm{opt},i}, \\ \frac{dp_i}{dI} &< 0 \quad \text{for } I > I_{\mathrm{opt},i} \end{aligned}$$

where $I_{\mathrm{opt},i}$ is the light intensity that attains the maximum specific production rate. A commonly used example of functions that satisfy the above conditions is (Fig. 1A):

$$p_i(I) = \frac{p_{\max,i} I}{\frac{p_{\max,i}}{\alpha_i I_{\mathrm{opt},i}^2} I^2 + (1 - 2\frac{p_{\max,i}}{\alpha_i I_{\mathrm{opt},i}}) I + \frac{p_{\max,i}}{\alpha_i}}, \tag{4}$$

where $p_{\max,i}$ is the maximum production rate and α_i is the initial slope of $p_i(I)$.

According to Gerla et al. (2011), we rewrite the depth-averaged production rate in (1). Substitution of variables yields

$$\frac{1}{z_{\max}} \int_0^{z_{\max}} p_i\big(I(z,t)\big)\,dz = \frac{1}{z_{\max}} \int_{I_{\mathrm{in}}}^{I_{\mathrm{out}}} p_i(I) \frac{\partial z}{\partial I}\,dI. \tag{5}$$

From (2), we have

$$\frac{\partial I}{\partial z} = -\left(\sum_{j=1}^{n} k_j x_j(t) \Big/ z_{\max} + K_{\mathrm{bg}}\right) I. \tag{6}$$

By substituting (6) into the right-hand side of (5), we obtain

$$\frac{1}{z_{\max}} \int_{I_{\mathrm{in}}}^{I_{\mathrm{out}}} p_i(I) \frac{\partial z}{\partial I}\, dI = \frac{1}{\sum_{j=1}^{n} k_j x_j(t) + K_{\mathrm{bg}} z_{\max}} \int_{I_{\mathrm{out}}}^{I_{\mathrm{in}}} \frac{p_i(I)}{I}\, dI. \tag{7}$$

We manipulate (3) and get

$$\ln(I_{\mathrm{in}}) - \ln(I_{\mathrm{out}}) = \sum_{j=1}^{n} k_j x_j(t) + K_{\mathrm{bg}} z_{\max}. \tag{8}$$

By substituting (8) into the right-hand side of (7), we have

$$\frac{1}{z_{\max}} \int_{0}^{z_{\max}} p_i\bigl(I(z,t)\bigr)\, dz = \frac{1}{\ln I_{\mathrm{in}} - \ln I_{\mathrm{out}}} \int_{I_{\mathrm{out}}}^{I_{\mathrm{in}}} \frac{p_i(I)}{I}\, dI. \tag{9}$$

We define the right-hand side of (9) to be $g_i(I_{\mathrm{out}})$, and the governing equation (1) becomes

$$\frac{dx_i}{dt} = \bigl[g_i\bigl(I_{\mathrm{out}}(t)\bigr) - d_i\bigr] x_i, \quad i = 1, 2, \ldots, n. \tag{10}$$

The function $g_i(I_{\mathrm{out}})$ satisfies $g_i(0) = 0$, $g_i(I_{\mathrm{in}}) = p_i(I_{\mathrm{in}})$. When $I_{\mathrm{in}} > I_{\mathrm{opt}}$, $g_i(I_{\mathrm{out}})$ is a unimodal function. In addition, when d_i is less than the maximum of $g_i(I_{\mathrm{out}})$, there are two points $I_{\mathrm{out}} = \lambda_i,\ \mu_i$ such that: $g_i(\lambda_i) = g_i(\mu_i) = d_i$; $g_i(I_{\mathrm{out}}) > d_i$ for $I_{\mathrm{out}} \in (\lambda_i, \mu_i)$; and $g_i(I_{\mathrm{out}}) < d_i$ for $I_{\mathrm{out}} \in [0, \lambda_i) \cup (\mu_i, \infty)$ (Fig. 1B; see the Appendix for the proof).

We define $I_0 := I_{\mathrm{in}} e^{-K_{\mathrm{bg}} z_{\max}}$, and then (3) is rewritten as

$$I_{\mathrm{out}}(t) = I_0 \exp\left(-\sum_{j=1}^{n} k_j x_j(t)\right). \tag{11}$$

We study (10) where $I_{\mathrm{out}}(t)$ is defined in (11) with the initial condition:

$$x_i(0) > 0 \quad \text{for } i = 1, 2, \ldots, n.$$

From the mathematical analysis, we prove that the solutions are positive and bounded, and that if $\lambda_i > I_0$, then the species i goes extinct as time t becomes large (see the Appendix). From now on, we simply assume

$$0 < \lambda_1 < \lambda_2 < \cdots < \lambda_n < I_0,$$

and $\mu_i \neq \mu_j, \lambda_j,\ I_0$ for $i \neq j$.

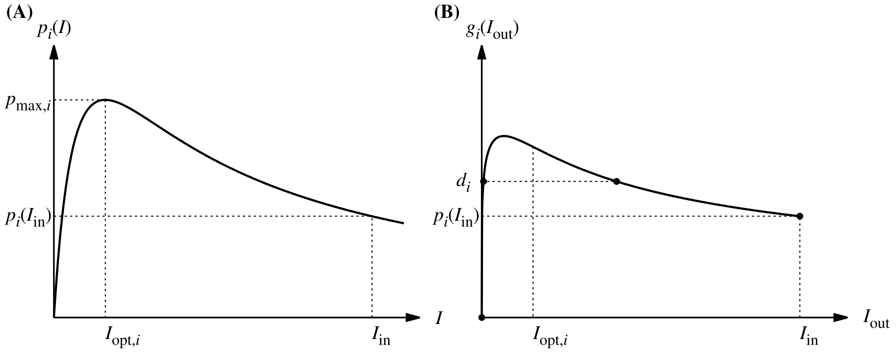

Fig. 1 (**A**) Specific production rate $p_i(I)$ of species i as a function of irradiance I expressed by Eq. (4). The curve has a peak at the optimal irradiance $I_{\mathrm{opt},i}$ with the maximum production rate $p_{\max,i}$. (**B**) The corresponding production rate averaged over the water column $g_i(I_{\mathrm{out}})$ as a function of I_{out}, irradiance at the bottom of the water column. Mathematical analysis shows $g_i(0) = 0$, $g_i(I_{\mathrm{in}}) = p_i(I_{\mathrm{in}})$, and that the curve has a peak at I_{out} which is lower than $I_{\mathrm{opt},i}$. When the loss rate d_i is lower than the maximum of g_i, there are λ_i and μ_i such that $g_i(\lambda_i) = g_i(\mu_i) = d_i$

First, we consider steady state of (10) and the local property. Steady state can be classified into three types:

$$\begin{aligned} E_0 &= (0, 0, \dots, 0); \\ E_{\lambda_r} &= (0, \dots, 0, x_{\lambda_r}, 0, \dots, 0), \quad r = 1, 2, \dots, n; \\ E_{\mu_r} &= (0, \dots, 0, x_{\mu_r}, 0, \dots, 0) \quad \text{for which } r \text{ satisfies } \mu_r < I_0, \end{aligned}$$

where x_{λ_r} and x_{μ_r} are expressed by

$$\begin{aligned} x_{\lambda_r} &= \frac{\ln I_0 - \ln \lambda_r}{k_r}, \\ x_{\mu_r} &= \frac{\ln I_0 - \ln \mu_r}{k_r}. \end{aligned}$$

For mathematical convenience, we introduce a positive cone

$$\Omega := \left\{ (x_1, x_2, \dots, x_n) \in \mathbb{R}^n : x_i > 0,\ i = 1, 2, \dots, n \right\}$$

and set S as

$$S := \bigcup_{i=1}^{n} (\lambda_i, \mu_i).$$

For some species i and j, intervals (λ_i, μ_i) and (λ_j, μ_j) may overlap. For example, if $\lambda_i < \lambda_j$ and $\mu_i < \mu_j$, the union will be (λ_i, μ_j). In a similar manner, S is expressed as a disjoint union of several connected components:

$$S = (\lambda_{p_1}, \mu_{q_1}) \cup (\lambda_{p_2}, \mu_{q_2}) \cup \cdots \cup (\lambda_{p_m}, \mu_{q_m}),$$

where m is the number of connected components, and λ_{p_j} and μ_{q_j}, respectively, are the left and right endpoints of component j ($j = 1, 2, \ldots, m$). In addition, we introduce two sets of steady state, S_L and S_R:

$$S_L = \{E_{\lambda_r} : \lambda_r \text{ is a left endpoint of components of } S\} \cup \{E_0\} \quad \text{if } I_0 \notin S,$$

$$S_R = \{E_{\mu_r} : \mu_r \text{ is a right endpoint of components of } S\}.$$

From linearization at steady state and the stability analysis, we can conclude that the local property is related to the structure of S (see the Appendix). The results are summarized as: steady state $E \in S_L$ is locally stable; $E \in S_R$ is saddle with $(n-1)$-dimensional stable manifold (denoted by $W^s(E)$ for $E \in S_R$), which intersects Ω; and other steady states are unstable, some of which are saddle with a stable manifold which does not intersect Ω.

By using mathematical methods similar to Butler and Wolkowicz (1985), we prove that $I_{\text{out}}(t)$ converges as t goes to infinity. Based on the result and local stability of steady state, we can describe the global behavior of system (10).

Theorem 1 *All solutions with initial condition in* $\Omega \backslash (\bigcup_{E \in S_R} W^s(E))$ *satisfy*

$$\lim_{t \to \infty} \bigl(x_1(t), x_2(t), \ldots, x_n(t)\bigr) = E \in S_L,$$

and the outcome depends on initial condition.

Theorem 1 tells us that all solutions from a positive initial condition converge to a steady state in the set S_L except when the initial condition lies in the stable manifold $W^s(E)$ with $E \in S_R$. The positive cone Ω is divided by $\bigcup_{E \in S_R} W^s(E)$ into several regions, and there is only one locally stable steady state $E \in S_L$ in each region that attracts all solutions with the initial condition in this region. These statements completely describe the global dynamics of the system investigated by Gerla et al. (2011), and assure that the competition outcomes can be evaluated from the structure of S and the position of I_0 for any number of species. We shall investigate some examples in the next section.

3 Feasibility of Theoretical Predictions

Gerla et al. (2011) showed diverse outcomes of 2-species competition including a strong Allee effect, competitive facilitation, and multiple positive alternative stable states. In this section, we demonstrate how mathematical properties of the system can be translated to ecological phenomena in 2- and 3-species competitions. Then we test feasibility of the theoretical predictions by applying empirical p–I curves to the model.

In order to classify competition outcomes, we suppose our basic assumption $\lambda_i < I_0$ holds for all species. Mathematical properties include the structure of S and the position of I_0 relative to S, the set of stable steady states, and the set of saddles with the stable manifold in Ω. The corresponding ecological phenom-

Table 1 Mathematical properties and ecological phenomena for the eight possible cases of 2-species competition. Mathematical properties shown in the table include structure of set S and the position of I_0 relative to S (Structure of S), set of stable steady states (Stable), and set of saddles with the stable manifold in Ω (Saddle). Ecological properties include a strong Allee effect (AL), competitive facilitation (FA), and the number of positive alternative stable states (ASS+)

	Structure of S		Stable	Saddle	AL	FA	ASS+
(A)	$(\lambda_1, \mu_1) \cup (\lambda_2, \mu_2)$;	$I_0 \notin S$	E_0, E_{λ_1}, E_{λ_2}	E_{μ_1}, E_{μ_2}	+	–	2
(B)	$(\lambda_1, \mu_1) \cup (\lambda_2, \mu_2)$;	$I_0 \in S$	E_{λ_1}, E_{λ_2}	E_{μ_1}	–	–	2
(C)	(λ_1, μ_2);	$I_0 \notin S$	E_0, E_{λ_1}	E_{μ_2}	+	2 → 1	–
(D)	(λ_1, μ_2);	$I_0 \in S$	E_{λ_1}	–	–	2 → 1	–
(E)	(λ_1, μ_2);	$I_0 \in S$	E_{λ_1}	–	–	–	–
(F)	(λ_1, μ_1);	$I_0 \notin S$	E_0, E_{λ_1}	E_{μ_1}	+	–	–
(G, H)	(λ_1, μ_1);	$I_0 \in S$	E_{λ_1}	–	–	–	–

ena include a strong Allee effect (AL), competitive facilitation (FA), and presence of positive alternative stable states (ASS+). AL is defined as the case when the system shows alternative stable states that include E_0 ($x_i = 0$ for all i). ASS+ is defined as the case when the system has multiple positive stable states. Therefore, alternative stable states consisting of only one positive state and E_0 do not belong to ASS+ but are captured by AL. FA is distinguished by the case when an interval of positive growth of a winning species overlaps, but does not completely cover, that of other species. In FA, a winning species i cannot persist in the system for some I_{out} where a losing species j can. As species j grows in the system and reduce I_{out}, species i eventually takes over the system. This case is described by $j \to i$ in tables. In 3-species competition, stable steady state may be achieved through a sequence of competitive facilitation such as: $3 \to 2 \to 1$.

For 2-species competition, we have the following eight cases:

(A) $\lambda_1 < \mu_1 < \lambda_2 < \mu_2 < I_0$
(B) $\lambda_1 < \mu_1 < \lambda_2 < I_0 < \mu_2$
(C) $\lambda_1 < \lambda_2 < \mu_1 < \mu_2 < I_0$
(D) $\lambda_1 < \lambda_2 < \mu_1 < I_0 < \mu_2$
(E) $\lambda_1 < \lambda_2 < I_0 < \mu_1 < \mu_2$
(F) $\lambda_1 < \lambda_2 < \mu_2 < \mu_1 < I_0$
(G) $\lambda_1 < \lambda_2 < \mu_2 < I_0 < \mu_1$
(H) $\lambda_1 < \lambda_2 < I_0 < \mu_2 < \mu_1$

Mathematical properties and the corresponding ecological phenomena for 2-species competition are summarized in Table 1. Based on backward trajectory and Theorem 1, we can describe the global behavior of the solutions of system (10) (Fig. 2). Note that the case (A) is equivalent to the intriguing case discussed in Fig. 6 of Gerla et al. (2011), where both species go extinct when they are initially abundant in the system (Fig. 2A).

For 3-species competition, we have the following 48 cases:

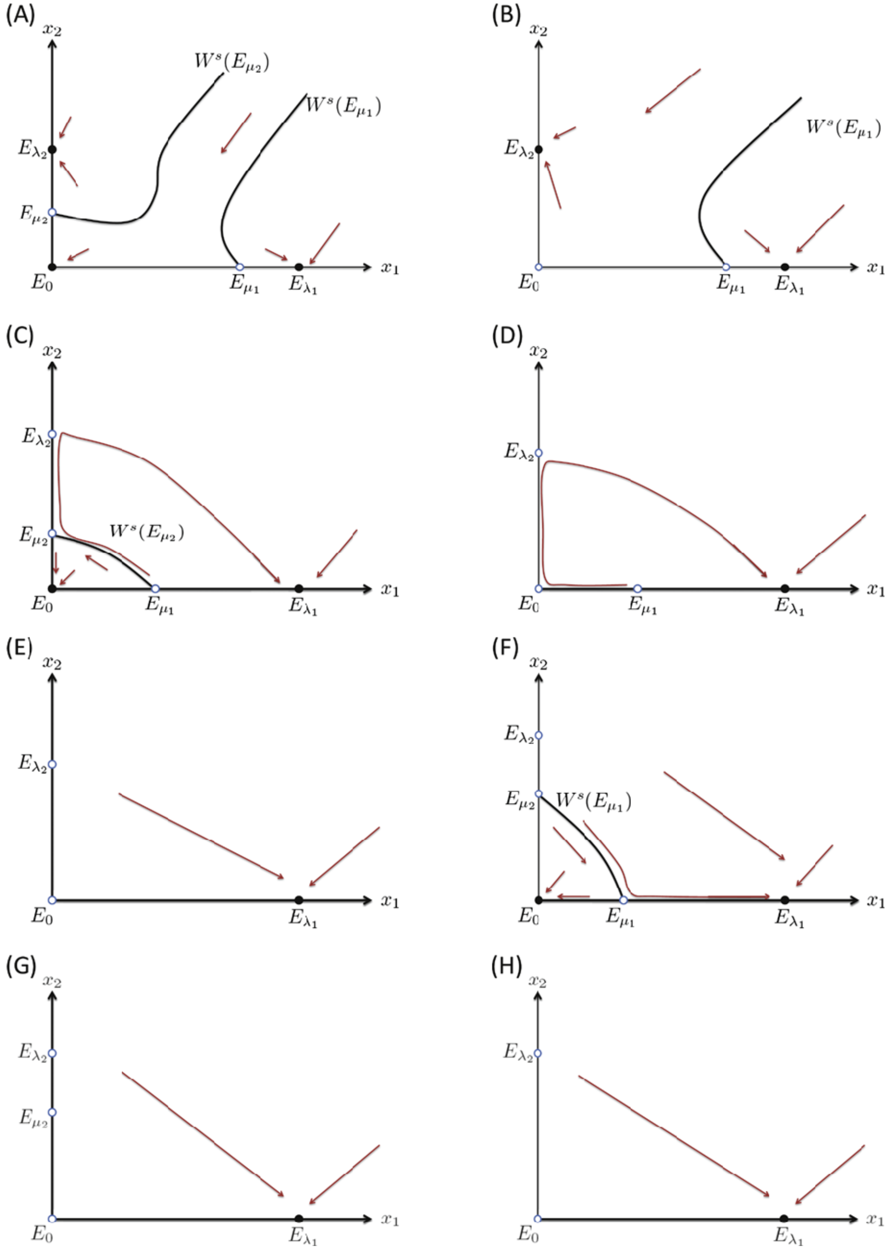

Fig. 2 Phase plane (x_1, x_2) depicts global behavior of 2-species competition. The *closed* and *open circles* are locally stable and unstable stable states, respectively. By reversing time, we draw the stable manifold of saddle point in the set S_L. (**A**) Two stable manifolds $W^s(E_{\mu_1})$ and $W^s(E_{\mu_2})$ separate the positive cone Ω into three parts, and there is an attractor in each part (E_0, E_{λ_1}, E_{λ_2}). (**B**) $W^s(E_{\mu_1})$ separates Ω into two parts, and there is an attractor $(E_{\lambda_1}, E_{\lambda_2})$ in each part. (**C**) $W^s(E_{\mu_1})$ separates Ω into two parts, and there is an attractor (E_0, E_{λ_1}) in each part. A heteroclinic orbit runs from E_{μ_1} to E_{μ_2} along $W^s(E_{\mu_1})$. (**D**, **E**, **G**, **H**) E_{λ_1} is a global attractor. (**F**) $W^s(E_{\mu_1})$ separates Ω into two parts, and there is an attractor (E_0, E_{λ_1}) in each part (Color figure online)

(A.1) $\lambda_1 < \mu_1 < \lambda_2 < \mu_2 < \lambda_3 < \mu_3 < I_0$
(A.2) $\lambda_1 < \mu_1 < \lambda_2 < \mu_2 < \lambda_3 < I_0 < \mu_3$
(B.1) $\lambda_1 < \mu_1 < \lambda_2 < \lambda_3 < \mu_2 < \mu_3 < I_0$
(B.2) $\lambda_1 < \mu_1 < \lambda_2 < \lambda_3 < \mu_2 < I_0 < \mu_3$
(B.3) $\lambda_1 < \mu_1 < \lambda_2 < \lambda_3 < I_0 < \mu_2 < \mu_3$
(C.1) $\lambda_1 < \mu_1 < \lambda_2 < \lambda_3 < \mu_3 < \mu_2 < I_0$
(C.2) $\lambda_1 < \mu_1 < \lambda_2 < \lambda_3 < \mu_3 < I_0 < \mu_2$
(C.3) $\lambda_1 < \mu_1 < \lambda_2 < \lambda_3 < I_0 < \mu_3 < \mu_2$
(D.1) $\lambda_1 < \lambda_2 < \mu_1 < \mu_2 < \lambda_3 < \mu_3 < I_0$
(D.2) $\lambda_1 < \lambda_2 < \mu_1 < \mu_2 < \lambda_3 < I_0 < \mu_3$
(E.1) $\lambda_1 < \lambda_2 < \mu_2 < \mu_1 < \lambda_3 < \mu_3 < I_0$
(E.2) $\lambda_1 < \lambda_2 < \mu_2 < \mu_1 < \lambda_3 < I_0 < \mu_3$
(F.1) $\lambda_1 < \lambda_2 < \mu_1 < \lambda_3 < \mu_2 < \mu_3 < I_0$
(F.2) $\lambda_1 < \lambda_2 < \mu_1 < \lambda_3 < \mu_2 < I_0 < \mu_3$
(F.3) $\lambda_1 < \lambda_2 < \mu_1 < \lambda_3 < I_0 < \mu_2 < \mu_3$
(G.1) $\lambda_1 < \lambda_2 < \mu_1 < \lambda_3 < \mu_3 < \mu_2 < I_0$
(G.2) $\lambda_1 < \lambda_2 < \mu_1 < \lambda_3 < \mu_3 < I_0 < \mu_2$
(G.3) $\lambda_1 < \lambda_2 < \mu_1 < \lambda_3 < I_0 < \mu_3 < \mu_2$
(H.1) $\lambda_1 < \lambda_2 < \mu_2 < \lambda_3 < \mu_3 < \mu_1 < I_0$
(H.2) $\lambda_1 < \lambda_2 < \mu_2 < \lambda_3 < \mu_3 < I_0 < \mu_1$
(H.3) $\lambda_1 < \lambda_2 < \mu_2 < \lambda_3 < I_0 < \mu_3 < \mu_1$
(I.1) $\lambda_1 < \lambda_2 < \mu_2 < \lambda_3 < \mu_1 < \mu_3 < I_0$
(I.2) $\lambda_1 < \lambda_2 < \mu_2 < \lambda_3 < \mu_1 < I_0 < \mu_3$
(I.3) $\lambda_1 < \lambda_2 < \mu_2 < \lambda_3 < I_0 < \mu_1 < \mu_3$
(J.1) $\lambda_1 < \lambda_2 < \lambda_3 < \mu_3 < \mu_2 < \mu_1 < I_0$
(J.2) $\lambda_1 < \lambda_2 < \lambda_3 < \mu_3 < \mu_2 < I_0 < \mu_1$
(J.3) $\lambda_1 < \lambda_2 < \lambda_3 < \mu_3 < I_0 < \mu_2 < \mu_1$
(J.4) $\lambda_1 < \lambda_2 < \lambda_3 < I_0 < \mu_3 < \mu_2 < \mu_1$
(K.1) $\lambda_1 < \lambda_2 < \lambda_3 < \mu_2 < \mu_3 < \mu_1 < I_0$
(K.2) $\lambda_1 < \lambda_2 < \lambda_3 < \mu_2 < \mu_3 < I_0 < \mu_1$
(K.3) $\lambda_1 < \lambda_2 < \lambda_3 < \mu_2 < I_0 < \mu_3 < \mu_1$
(K.4) $\lambda_1 < \lambda_2 < \lambda_3 < I_0 < \mu_2 < \mu_3 < \mu_1$
(L.1) $\lambda_1 < \lambda_2 < \lambda_3 < \mu_2 < \mu_1 < \mu_3 < I_0$
(L.2) $\lambda_1 < \lambda_2 < \lambda_3 < \mu_2 < \mu_1 < I_0 < \mu_3$
(L.3) $\lambda_1 < \lambda_2 < \lambda_3 < \mu_2 < I_0 < \mu_1 < \mu_3$
(L.4) $\lambda_1 < \lambda_2 < \lambda_3 < I_0 < \mu_2 < \mu_1 < \mu_3$
(M.1) $\lambda_1 < \lambda_2 < \lambda_3 < \mu_1 < \mu_2 < \mu_3 < I_0$
(M.2) $\lambda_1 < \lambda_2 < \lambda_3 < \mu_1 < \mu_2 < I_0 < \mu_3$
(M.3) $\lambda_1 < \lambda_2 < \lambda_3 < \mu_1 < I_0 < \mu_2 < \mu_3$
(M.4) $\lambda_1 < \lambda_2 < \lambda_3 < I_0 < \mu_2 < \mu_1 < \mu_3$
(N.1) $\lambda_1 < \lambda_2 < \lambda_3 < \mu_3 < \mu_1 < \mu_2 < I_0$
(N.2) $\lambda_1 < \lambda_2 < \lambda_3 < \mu_3 < \mu_1 < I_0 < \mu_2$
(N.3) $\lambda_1 < \lambda_2 < \lambda_3 < \mu_3 < I_0 < \mu_1 < \mu_2$
(N.4) $\lambda_1 < \lambda_2 < \lambda_3 < I_0 < \mu_3 < \mu_1 < \mu_2$
(O.1) $\lambda_1 < \lambda_2 < \lambda_3 < \mu_1 < \mu_3 < \mu_2 < I_0$
(O.2) $\lambda_1 < \lambda_2 < \lambda_3 < \mu_1 < \mu_3 < I_0 < \mu_2$
(O.3) $\lambda_1 < \lambda_2 < \lambda_3 < \mu_1 < I_0 < \mu_3 < \mu_2$
(O.4) $\lambda_1 < \lambda_2 < \lambda_3 < I_0 < \mu_1 < \mu_3 < \mu_2$

Mathematical properties and the corresponding ecological phenomena for 3-species competition are summarized in Table 2. Based on the mathematical analysis, we can exactly describe the global behavior. We will not present each of 48 cases, but classify all cases by the number of attractors and the structure of stable manifold of saddle in Ω, resulting in 8 classical types (Fig. 3).

As we have seen in 2- and 3-species cases, the light competition model with photoinhibition shows a variety of dynamical behaviors. In order to evaluate feasibility of these theoretical predictions, we applied empirical p–I curves to the model. In Schwaderer et al. (2011) compiled empirical data of specific growth rate and irradiance relationships for 56 phytoplankton species. Among them, relationships for 39 species indicated photoinhibition, and were fitted by Eq. (4). We considered these 39 species for our numerical experiments. The maximum production rate $p_{\max,i}$ (d^{-1}) of the species ranged from 0.09 to 2.48 with a median of 0.64; the initial slope α_i (μmol photon^{-1} m^2 s d^{-1}), ranged from 0.003 to 0.099 with a median of 0.015; and the optimal irradiance $I_{\mathrm{opt},i}$ (μmol photon m^{-2} s^{-1}) ranged from 37.5 to 250.8 with a median of 161.5. In numerical experiments, we set model parameters to combinations of low or high loss rate ($d_i = 0.25$, 0.5 [d^{-1}]), and low, high, or a range of incident light ($I_{\mathrm{in}} = 500$, 1500, 0–2000 [μmol photon m^{-2} s^{-1}]) in a clear ($K_{\mathrm{bg}} = 0.2$ [m^{-1}]) and shallow ($z_{\max} = 1$ [m]) water column.

Positive growth intervals (λ_i, μ_i) are computed for the 39 species. Several species cannot grow for any I_{out} at $d = 0.25$ due to the low $p_{\max,i}$ (Figs. 4AB). Positive growth intervals of two species (*Scenedesmus crassus* and *Chlorella pyrenoidosa*) ranged from $<10^{-4}$ to I_{in} due to the high $p_{\max,i}$ (1.29 and 2.48) and the relatively high α_i (0.042 and 0.045). Among species that can grow for some I_{out}, several species

Table 2 Mathematical properties and ecological phenomena for all possible cases of 3-species competition. Notation follows Table 1

	Structure of S		Stable	Saddle	AL	FA	ASS+
(A.1)	$(\lambda_1,\mu_1)\cup(\lambda_2,\mu_2)\cup(\lambda_3,\mu_3)$;	$I_0\notin S$	$E_0, E_{\lambda_1}, E_{\lambda_2}, E_{\lambda_3}$	$E_{\mu_1}, E_{\mu_2}, E_{\mu_3}$	+	–	3
(A.2)	$(\lambda_1,\mu_1)\cup(\lambda_2,\mu_2)\cup(\lambda_3,\mu_3)$;	$I_0\in S$	$E_{\lambda_1}, E_{\lambda_2}, E_{\lambda_3}$	E_{μ_1}, E_{μ_2}	–	–	3
(B.1)	$(\lambda_1,\mu_1)\cup(\lambda_2,\mu_3)$;	$I_0\notin S$	$E_0, E_{\lambda_1}, E_{\lambda_2}$	E_{μ_1}, E_{μ_3}	+	$3\to 2$	2
(B.2)	$(\lambda_1,\mu_1)\cup(\lambda_2,\mu_3)$;	$I_0\in S$	$E_{\lambda_1}, E_{\lambda_2}$	E_{μ_1}	–	$3\to 2$	2
(B.3)	$(\lambda_1,\mu_1)\cup(\lambda_2,\mu_3)$;	$I_0\in S$	$E_{\lambda_1}, E_{\lambda_2}$	E_{μ_1}	–	–	2
(C.1)	$(\lambda_1,\mu_1)\cup(\lambda_2,\mu_2)$;	$I_0\notin S$	$E_0, E_{\lambda_1}, E_{\lambda_2}$	E_{μ_1}, E_{μ_2}	+	–	2
(C.2–3)	$(\lambda_1,\mu_1)\cup(\lambda_2,\mu_2)$;	$I_0\in S$	$E_{\lambda_1}, E_{\lambda_2}$	E_{μ_1}	–	–	2
(D.1)	$(\lambda_1,\mu_2)\cup(\lambda_3,\mu_3)$;	$I_0\notin S$	$E_0, E_{\lambda_1}, E_{\lambda_3}$	E_{μ_2}, E_{μ_3}	+	$2\to 1$	2
(D.2)	$(\lambda_1,\mu_2)\cup(\lambda_3,\mu_3)$;	$I_0\in S$	$E_{\lambda_1}, E_{\lambda_3}$	E_{μ_2}	–	$2\to 1$	2
(E.1)	$(\lambda_1,\mu_1)\cup(\lambda_3,\mu_3)$;	$I_0\notin S$	$E_0, E_{\lambda_1}, E_{\lambda_3}$	E_{μ_1}, E_{μ_3}	+	–	2
(E.2)	$(\lambda_1,\mu_1)\cup(\lambda_3,\mu_3)$;	$I_0\in S$	$E_{\lambda_1}, E_{\lambda_3}$	E_{μ_1}	–	–	2
(F.1)	(λ_1,μ_3);	$I_0\notin S$	E_0, E_{λ_1}	E_{μ_3}	+	$3\to 2\to 1$	–
(F.2)	(λ_1,μ_3);	$I_0\in S$	E_{λ_1}	–	–	$3\to 2\to 1$	–
(F.3)	(λ_1,μ_3);	$I_0\in S$	E_{λ_1}	–	–	$2\to 1$	–
(G.1)	(λ_1,μ_2);	$I_0\notin S$	E_0, E_{λ_1}	E_{μ_2}	+	$2\to 1$	–
(G.2–3)	(λ_1,μ_2);	$I_0\in S$	E_{λ_1}	–	–	$2\to 1$	–
(H.1)	(λ_1,μ_1);	$I_0\notin S$	E_0, E_{λ_1}	E_{μ_1}	+	–	–
(H.2–3)	(λ_1,μ_1);	$I_0\in S$	E_{λ_1}	–	–	–	–
(I.1)	(λ_1,μ_3);	$I_0\notin S$	E_0, E_{λ_1}	E_{μ_3}	+	$3\to 1$	–
(I.2)	(λ_1,μ_3);	$I_0\in S$	E_{λ_1}	–	–	$3\to 1$	–
(I.3)	(λ_1,μ_3);	$I_0\in S$	E_{λ_1}	–	–	–	–
(J.1)	(λ_1,μ_1);	$I_0\notin S$	E_0, E_{λ_1}	E_{μ_1}	+	–	–
(J.2–4)	(λ_1,μ_1);	$I_0\in S$	E_{λ_1}	–	–	–	–
(K.1)	(λ_1,μ_1);	$I_0\notin S$	E_0, E_{λ_1}	E_{μ_1}	+	–	–
(K.2–4)	(λ_1,μ_1);	$I_0\in S$	E_{λ_1}	–	–	–	–
(L.1)	(λ_1,μ_3);	$I_0\notin S$	E_0, E_{λ_1}	E_{μ_3}	+	$3\to 1$	–
(L.2)	(λ_1,μ_3);	$I_0\in S$	E_{λ_1}	–	–	$3\to 1$	–
(L.3–4)	(λ_1,μ_3);	$I_0\in S$	E_{λ_1}	–	–	–	–
(M.1)	(λ_1,μ_3);	$I_0\notin S$	E_0, E_{λ_1}	E_{μ_3}	+	$3\to 1$	–
(M.2)	(λ_1,μ_3);	$I_0\in S$	E_{λ_1}	–	–	$3\to 1$	–
(M.3)	(λ_1,μ_3);	$I_0\in S$	E_{λ_1}	–	–	(2 or 3) → 1	–
(M.4)	(λ_1,μ_3);	$I_0\in S$	E_{λ_1}	–	–	–	–
(N.1)	(λ_1,μ_2);	$I_0\notin S$	E_0, E_{λ_1}	E_{μ_2}	+	$2\to 1$	–
(N.2)	(λ_1,μ_2);	$I_0\in S$	E_{λ_1}	–	–	$2\to 1$	–
(N.3–4)	(λ_1,μ_2);	$I_0\in S$	E_{λ_1}	–	–	–	–
(O.1)	(λ_1,μ_2);	$I_0\notin S$	E_0, E_{λ_1}	E_{μ_2}	+	$2\to 1$	–
(O.2–3)	(λ_1,μ_2);	$I_0\in S$	E_{λ_1}	–	–	$2\to 1$	–
(O.4)	(λ_1,μ_2);	$I_0\in S$	E_{λ_1}	–	–	–	–

showed a strong Allee effect at $d = 0.25$ and $I_{\text{in}} = 500$ (Fig. 4A). On the other hand, most species showed a strong Allee effect (Figs. 4BCD) at high loss rate $d = 0.5$ and/or high incoming light $I_{\text{in}} = 1500$.

The intriguing ecological phenomena such as AL, ASS+, and FA were observed in the numerical experiments. For example, when *Limnothrix redekei* and *Fragilaria rumpens* compete under low light (500 μmol photon $\text{m}^{-2}\ \text{s}^{-1}$) and high loss rate

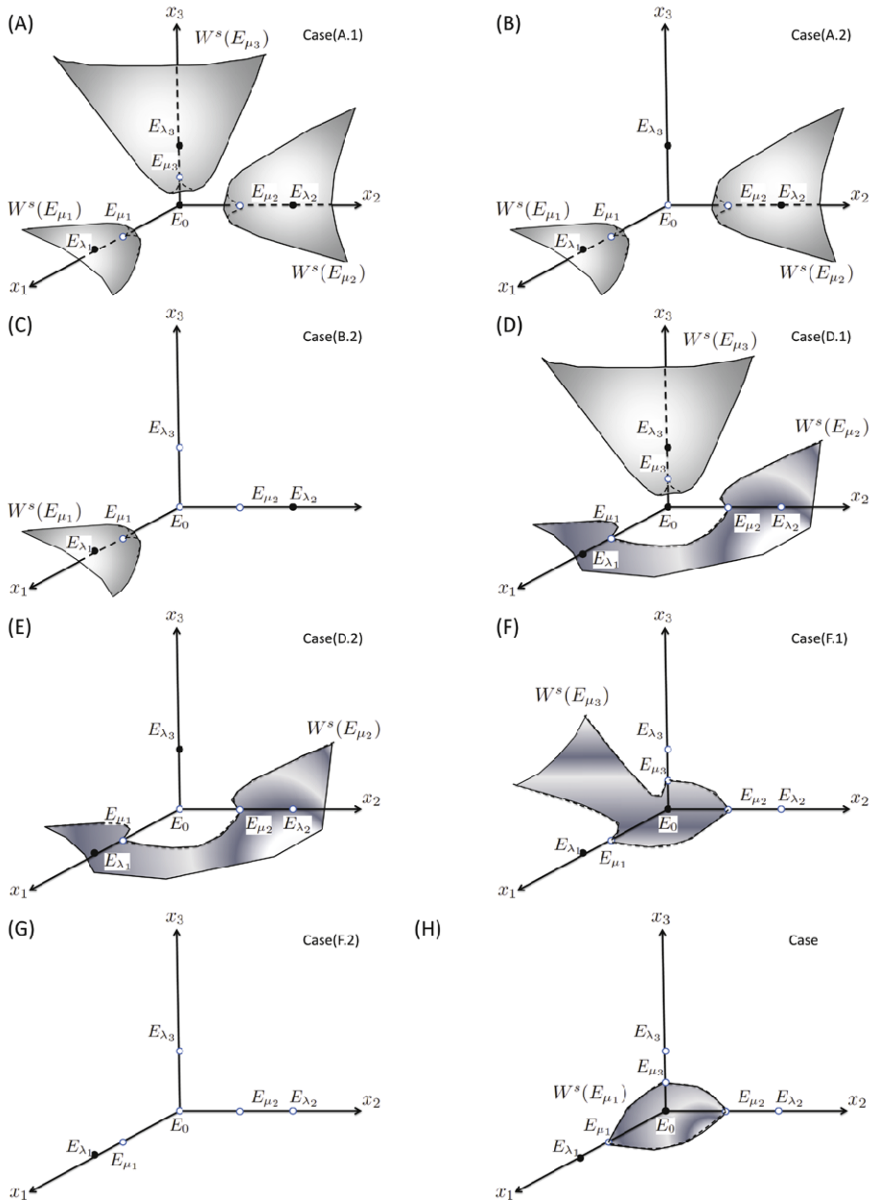

Fig. 3 Phase plane (x_1, x_2, x_3) depicts global behavior of 3-species competition. The *closed* and the *open circles* are locally stable and unstable steady states, respectively. Based on the structure of 2-species cases, we can describe the behavior on the boundary planes of Ω. (**A**) $W^s(E_{\mu_1})$, $W^s(E_{\mu_2})$ and $W^s(E_{\mu_3})$ separate Ω into four parts, and there is an attractor $(E_0, E_{\lambda_1}, E_{\lambda_2}, E_{\lambda_3})$ in each part. (**B**) $W^s(E_{\mu_1})$ and $W^s(E_{\mu_2})$ separate Ω into three parts, there is an attractor $(E_{\lambda_1}, E_{\lambda_2}, E_{\lambda_3})$ in each part. (**C**) $W^s(E_{\mu_1})$ separates Ω into two parts, and there is an attractor $(E_{\lambda_1}, E_{\lambda_2})$ in each part. (**D**) $W^s(E_{\mu_2})$ and $W^s(E_{\mu_3})$ separates Ω into three parts, and there is an attractor $(E_0, E_{\lambda_1}, E_{\lambda_3})$ in each part. (**E**) $W^s(E_{\mu_1})$ separates Ω into two parts, and there is an attractor $(E_{\lambda_1}, E_{\lambda_3})$ in each part. (**F**) $W^s(E_{\mu_3})$ separates Ω into two parts, there is an attractor (E_0, E_{λ_1}) in each part. (**G**) E_{λ_1} is a globally attractor. (**H**) $W^s(E_{\mu_1})$ separates Ω into two parts, and there is an attractor (E_0, E_{λ_1}) in each part

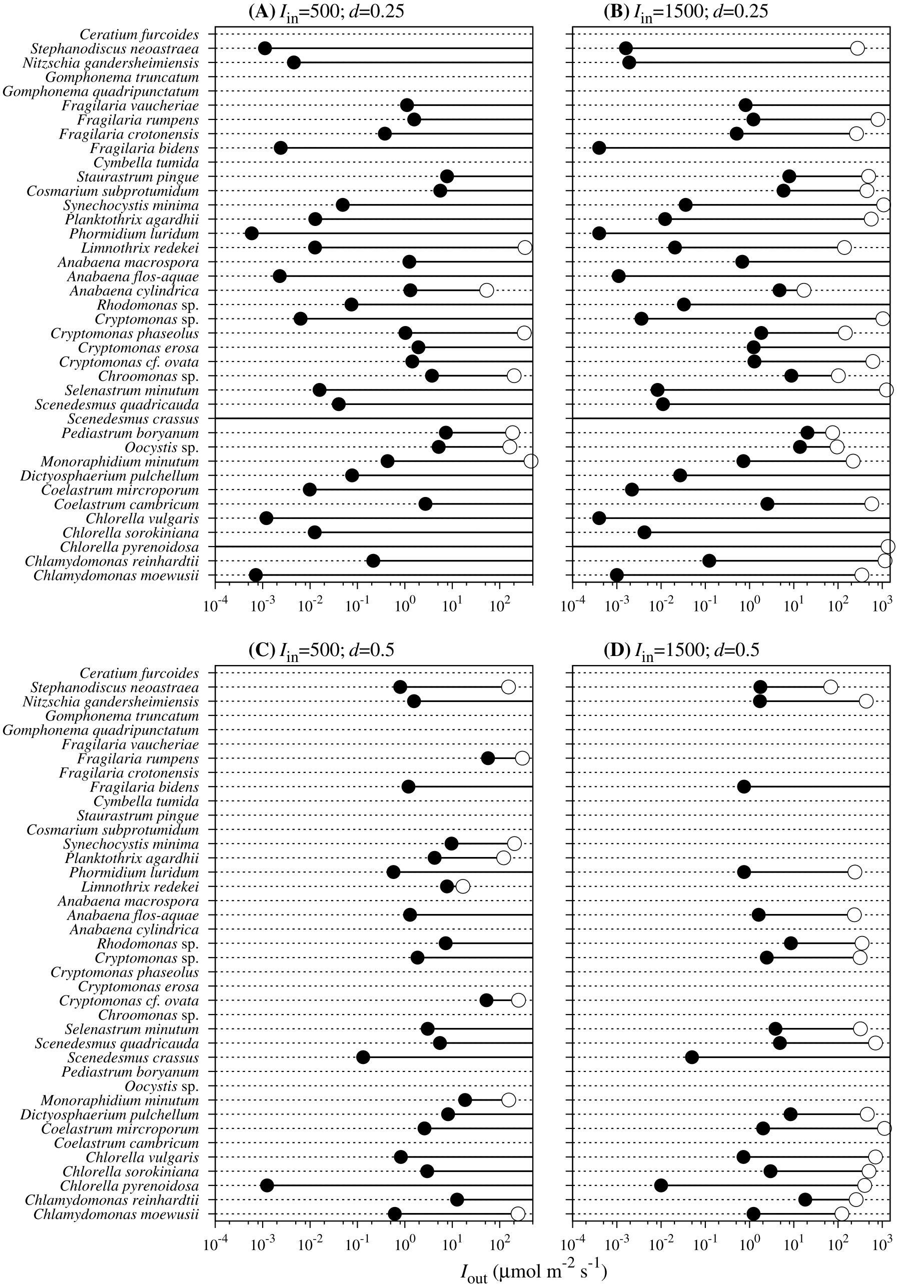

Fig. 4 Ranges of I_{out} with positive net production are depicted for 39 species that exhibit photoinhibition. *Closed* and *open circles* indicate stable and unstable steady states, respectively. *Solid lines* indicate intervals where net production is positive. *Dotted lines* indicate intervals where net production is negative. (**A**) Low light ($I_{\text{in}} = 500$) and low loss rate ($d = 0.25$) condition. (**B**) High light ($I_{\text{in}} = 1500$) and low loss rate condition. (**C**) Low light and high loss rate ($d = 0.5$) condition. (**D**) High light and high loss rate conditions. Species with both *closed* and *open circles* show a strong Allee effect

($0.5\ \mathrm{d}^{-1}$) condition, the competition outcome is either that both species go extinct, or that one of the two species persists depending on the initial condition (Fig. 5A). This case corresponds to (A) of Table 1 and is classified as AL and ASS+. When *Stephanodiscus neoastraea* and *Rhodomonas* sp. were grown together under low light and high loss rate condition from low initial biomasses, *Rhodomonas* sp. grew first, and was eventually replaced by *S. neoastraea* (Fig. 5B). This case corresponds to (D) of Table 1 and is classified as FA, (*Rhodomonas* sp.)→(*S. neoastraea*), where the latter species cannot grow from the low initial biomass by itself.

Figure 6 shows feasibility of theoretical predictions along the gradient of incoming light I_{in} with an increment $\Delta I_{\mathrm{in}} = 1$. In monoculture, a species either goes extinct, persists regardless of the initial condition with the biomass converge to a positive global attractor, or shows a strong Allee effect (Figs. 6AB). The number of species whose biomass converges to a positive global attractor has a peak around the median of I_{opt}, and the number of species that shows a strong Allee effect increases with increasing I_{in}. The trends are similar for $d = 0.25$ and $d = 0.5$. In 2- and 3-species competitions, we consider combinations of species that have a positive growth interval in monoculture for a given I_{in}. For 2-species competition, we classified the competition outcomes as in Table 1. For 3-species competition, FA is distinguished whether 1 or 2 species play roles in facilitation (FA(1) and FA(2)), and ASS+, by the number of positive stable states (ASS+(2) and ASS+(3)). For each case of competition outcomes, we computed the number of combinations relative to the total number of combinations of species with a positive growth interval for a given I_{in}. When $d = 0.25$, the relative number of combinations that indicated FA and AL showed increasing trends with I_{in} while ASS+ was not observed in both 2- and 3-species competitions (Figs. 6CE). When $d = 0.5$, FA and AL showed similar increasing trends, and ASS+ was observed in a few combinations at relatively low I_{in} (Figs. 6DF). For 3-species competition, 3 positive alternative stable states ASS+(3) and sequential facilitation FA(2) were also possible in several combinations.

When $d = 0.25$ and $d = 0.5$, about 60 % and 40 % of species showed an strong Allee effect at high I_{in} (Figs. 6AB), which is >70 % and >80 % of species that have a positive growth interval, respectively. As a result, a strong Allee effect is common in 2- and 3-species competition at high I_{in} (Figs. 6CDEF). FA is commonly observed as well, about 25 % and 50 %, respectively, when $d = 0.25$ and $d = 0.5$ in both 2- and 3-species competitions (Figs. 6CDEF). Facilitation by more than one species was observed only in a few cases when $d = 0.5$ at relatively low I_{in} (Fig. 6F). ASS+ was not observed except for very limited combinations when $d = 0.5$ (Figs. 6DF). These phenomena are less likely to occur in more turbid and deeper water (results not shown).

4 Discussion

In this study, we analyzed the dynamical behavior of a light competition model with photoinhibition proposed by Huisman (1997) and Gerla et al. (2011). We proved that light at the bottom of the water column $I_{\mathrm{out}}(t)$ converges as t goes to infinity, which excludes possibility of limit cycle, and hence excludes possibility of coexistence in

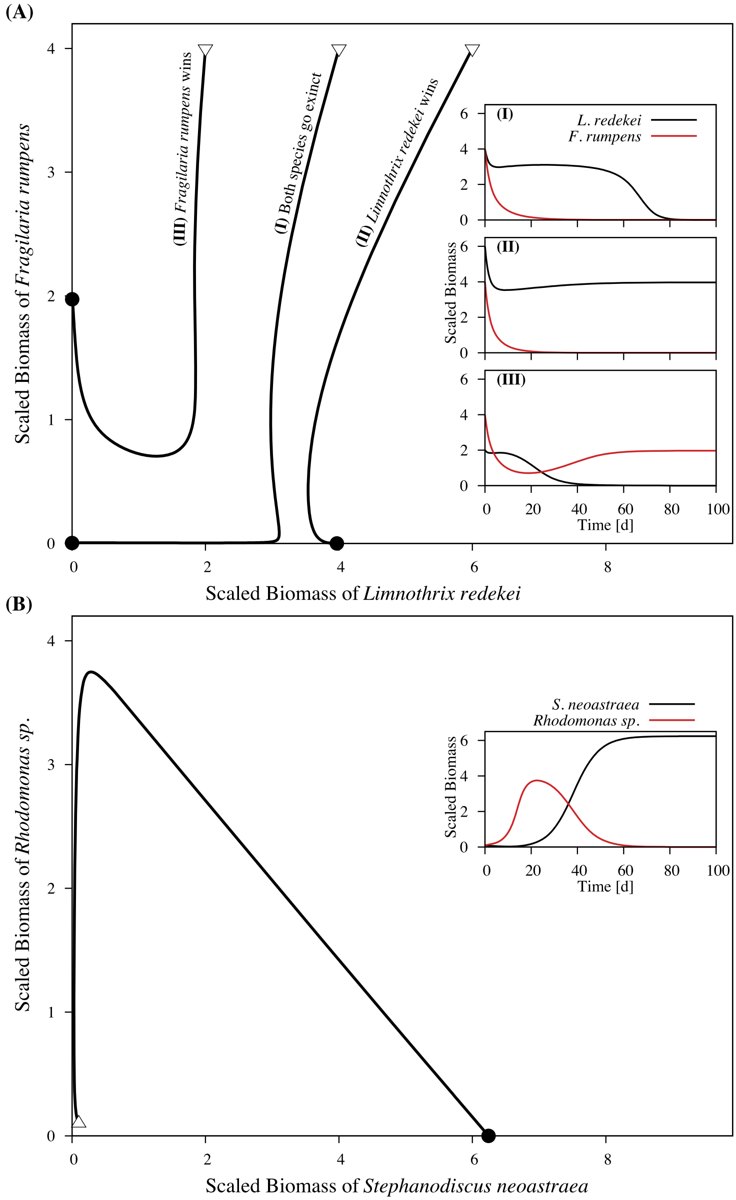

Fig. 5 Trajectories of the 2-species competition on phase plane, and the corresponding time courses in the *inset panels*. Biomasses shown in figures are multiplied by the specific light attenuation coefficient ($k_i x_i$). The *open triangle* and the *closed circle* on each trajectory indicate the initial condition and the stable steady state, respectively. (**A**) Competition between *Limnothrix redekei* and *Fragilaria rumpens*. Parameters of p–I curves can be found in Schwaderer et al. (2011). Other parameters are: $I_{\text{in}} = 500$, $d_1 = d_2 = 0.5$, $z_{\max} = 1$, and $K_{\text{bg}} = 0.2$. The competition outcome is either (*I*) both species go extinct, (*II*) *L. redekei* wins, or (*III*) *F. rumpens* wins, depending on the initial condition. (**B**) Competition between *Stephanodiscus neoastraea* and *Rhodomonas* sp. Parameters are the same as in (**A**). When the initial biomasses are small, *Rhodomonas* sp. increases first, and subsequently outcompeted by *S. neoastraea* (Color figure online)

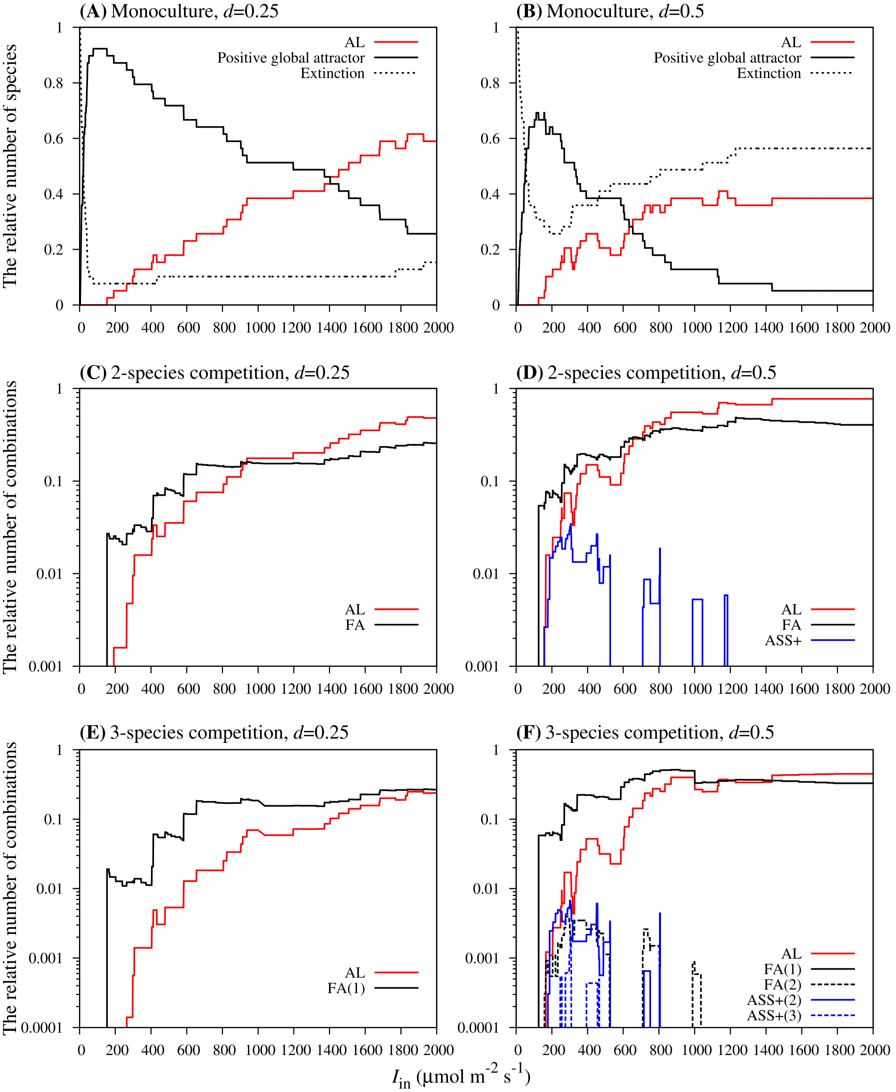

Fig. 6 Results of numerical experiments. Monoculture growth with low (**A**) and high (**B**) loss rates; 2-species competition with low (**C**) and high (**D**) loss rates; and 3-species competition with low (**E**) and high (**F**) loss rates. Other model parameters are: $K_{\mathrm{bg}} = 0.2$ and $z_{\max} = 1$. Outcomes are evaluated by the relative number of species or species combinations for each I_{in}. *AL* indicates a strong Allee effect, *FA*, competitive facilitation, and *ASS*+, presence of multiple positive stable states. In 3-species competition, *FA* is distinguished by the number of species that participate in the facilitation, and *ASS*+, by the number of positive stable states (Color figure online)

competition between any number of species. This property is similar to the model without photoinhibition (proof was given by Weissing and Huisman 1994). Theorem 1 states that the positive cone Ω is separated into regions by the stable manifolds of saddle points in the set S_R. In each region, there is only one stable steady state in the set S_L, which attracts all trajectories in the region. Therefore, there are alternative stable states and the competition outcomes depend on the initial conditions. Our mathematical results are consistent with results of Gerla et al. (2011), and augment them by a more general theory and analytical approach to the question of light competition with photoinhibition. In addition, we employed empirical p–I curves, and evaluated feasibility of the theoretical predictions.

Resources are beneficial at the limiting amount, yet occasionally show inhibitory effects on growth when supplied at the excessive amount. Indeed, inorganic and organic nutrients can be inhibitory at the high concentrations. Resource competition models that incorporate inhibitory effects of nutrients were proposed by Andrews (1968) and rigorously analyzed by Butler and Wolkowicz (1985). Such high nutrient concentrations are rarely observed, however, except for artificially fertilized environments or for a few specific species in typical *in situ* conditions. Light, on the other hand, can be inhibitory in normal conditions for all phototrophs, thus the inhibitory effects are relevant to ecosystem processes. Yet, effects of photoinhibition on light competition and community structure are not well understood, and most ecological theories of light competition do not consider photoinhibition. This study, in concert with Gerla et al. (2011), gives fundamental theory of light competition with photoinhibition.

Inhibitory effects by excessive amount of resources cause a strong Allee effect, alternative stable steady states, and competitive facilitation in resource competition models (Butler and Wolkowicz 1985; Gerla et al. 2011). Our numerical experiments suggest that a strong Allee effect and competitive facilitation are common in competition for light when we consider empirical p–I curves (Fig. 6). The influence of photoinhibition may be more severe in natural phytoplankton communities. Empirical p–I curves are obtained in nutrient replete conditions at temperature around 20 °C. Because recovery from photodamages largely depends on the nutritional conditions of cells as well as the ambient temperature (Bouchard et al. 2006; Muller 2010), phytoplankton species may be more susceptible to strong light in field conditions. In addition, fluorescent lamps used in experiments do not emit as much ultraviolet (UV, 290–400 nm in wavelength) radiation as sunlight, while UV radiation exerts greater photodamages than photosynthetically available radiation (PAR, 400–700 nm) (Bouchard et al. 2006). With exposure to UV in addition to PAR, phytoplankton species may show lower maximum growth rate $p_{\max}$ and optimal irradiance I_{opt} (Litchman et al. 2002; Litchman and Neale 2005). On the other hand, we exclusively considered species that show photoinhibition in our numerical experiment. Such selection of species may result in overestimation of the effect of photoinhibition on phytoplankton communities. However, we think this selection is fair, though not the best, because most p–I relationships were not evaluated at high irradiance levels where photosynthesis is inhibited and photoinhibition is detected (Schwaderer et al. 2011). Thus, we conclude that photoinhibition takes an important role in shaping phytoplankton community structure.

Our mathematical analysis confirmed that coexistence is not possible in competition for light with photoinhibition in a well-mixed water column. For coexistence of species, we need to consider additional factors. For example, differential responses of phytoplankton to different wavelengths of PAR (Stomp et al. 2007) and of UV (Litchman et al. 2002; Litchman and Neale 2005) are possibilities. Incomplete mixing of a water column may allow niche segregation along the light gradient (Yoshiyama et al. 2009). Including a limiting nutrient to the model (Huisman and Weissing 1995), vertically heterogeneous mixing (Yoshiyama and Nakajima 2002; Ryabov et al. 2010; Mellard et al. 2011), or taxis behavior (Klausmeier and Litchman 2001) are possible extensions to the light competition model with photoinhibition.

Trait-based approaches are being increasingly used to explain community organization along various environmental gradients in both terrestrial and aquatic ecology (McGill et al. 2006; Litchman and Klausmeier 2008). Light utilization traits are considered to be among the primary factors that structure plant communities (Kohyama 1993; Huisman and Weissing 1994; Schwaderer et al. 2011). Among the light utilization traits, photoinhibition has been dismissed in theoretical ecology. Our study attempted to evaluate whether photoinhibition has significant effects on phytoplankton community ecology through mathematical analysis and numerical experiments of a light competition model. Our numerical experiment showed that a strong Allee effect and competitive facilitation are commonly observed in 2- and 3-species competitions, and indicated such specific ecological phenomena to inhibitory responses to strong light may be common in natural phytoplankton communities. Our results, in turn, suggest the need for better empirical and theoretical understandings of physiological responses to light along environmental gradients in order to elucidate phytoplankton community structure.

Acknowledgements We are grateful to Jef Huisman and an anonymous referee for their helpful comments and suggestions which led to an improvement of our original manuscript. Kohei Yoshiyama would like to thank the National Center for Theoretical Science, National Tsing-Hua University, Taiwan, for its financial support and kind hospitality during his visit there.

Appendix

A.1 Basic Properties

We will demonstrate the shape of function

$$g(x) = \frac{1}{\ln I_{\mathrm{in}} - \ln x} \int_x^{I_{\mathrm{in}}} \frac{p(I)}{I}\, dI \quad \text{for } x \in [0, I_{\mathrm{in}}],$$

where $p(I)$ satisfies $p(0) = 0$, $p(I) \in (0, \infty)$ for $0 < I \leq I_{\mathrm{in}}$, $dp/dI < \infty$, $dp/dI > 0$ for $0 \leq I < I_{\mathrm{opt}}$, and $dp/dI < 0$ for $I_{\mathrm{opt}} < I \leq I_{\mathrm{in}}$. We claim that $g(0) = 0$ and $g(I_{\mathrm{in}}) = p(I_{\mathrm{in}})$, and there is a unique point $\hat{x}$ such that $dg(\hat{x})/dx = 0$, and $dg/dx > 0$ for $x \in [0, \hat{x})$; $dg/dx < 0$ for $x \in (\hat{x}, I_{\mathrm{in}}]$.

The proof of $g(0) = 0$ is straightforward:

$$\lim_{x \to 0} g(x) = \int_0^{I_{\mathrm{in}}} \frac{p(I)}{I}\, dI \lim_{x \to 0} \frac{1}{\ln I_{\mathrm{in}} - \ln x} = 0,$$

because $\int_0^{I_{\text{in}}} \frac{p(I)}{I}\,dI$ is bounded and $\lim_{x\to 0}(\ln I_{\text{in}} - \ln x) = \infty$. Likewise, $g(I_{\text{in}}) = p(I_{\text{in}})$ can be proved by

$$\lim_{x\to I_{\text{in}}} g(x) = \lim_{x\to I_{\text{in}}} \frac{\int_x^{I_{\text{in}}} \frac{p(I)}{I}\,dI}{\ln I_{\text{in}} - \ln x} = \lim_{x\to I_{\text{in}}} \frac{-\frac{p(x)}{x}}{-\frac{1}{x}} = \lim_{x\to I_{\text{in}}} p(x) = p(I_{\text{in}}).$$

Next, we prove that $g(x)$ is a unimodal function with a peak at $\hat{x} \in (0, I_{\text{opt}})$. The derivative of $g(x)$ is

$$\begin{aligned}\frac{dg}{dx} &= \frac{1}{(\ln I_{\text{in}} - \ln x)^2}\left[-\frac{p(x)}{x}(\ln I_{\text{in}} - \ln x) + \frac{1}{x}\int_x^{I_{\text{in}}} \frac{p(I)}{I}\,dI\right]\\ &= \frac{1}{(\ln I_{\text{in}} - \ln x)^2 x}\left[-p(x)(\ln I_{\text{in}} - \ln x) + \int_x^{I_{\text{in}}} \frac{p(I)}{I}\,dI\right].\end{aligned}$$

Let

$$\begin{aligned} g_1(x) &= p(x)(\ln I_{\text{in}} - \ln x) \geq 0,\\ g_2(x) &= \int_x^{I_{\text{in}}} \frac{p(I)}{I}\,dI \geq 0,\end{aligned}$$

Because $p(0) = 0$ from the assumption, we have

$$\begin{aligned}\lim_{x\to 0} g_1(x) = \lim_{x\to 0} p(x)(\ln I_{\text{in}} - \ln x) &= \lim_{x\to 0} \frac{\ln I_{\text{in}} - \ln x}{\frac{1}{p(x)}}\\ &= \lim_{x\to 0} \frac{-\frac{1}{x}}{-\frac{p'(x)}{p^2(x)}} = \lim_{x\to 0} \frac{\frac{p(x)}{x}}{p'(x)} p(x) = 0.\end{aligned}$$

Therefore, $g_1(0) < g_2(0)$ and $g_1(I_{\text{in}}) = g_2(I_{\text{in}}) = 0$.

The derivatives of $g_1(x)$ and $g_2(x)$ are:

$$g_1'(x) = p'(x)(\ln I_{\text{in}} - \ln x) - \frac{p(x)}{x}, \tag{12}$$

$$g_2'(x) = -\frac{p(x)}{x}. \tag{13}$$

Because $p'(x) < 0$ for $x \in (I_{\text{opt}}, I_{\text{in}}]$, we have $|g_1'(I_{\text{in}}^-)| > |g_2'(I_{\text{in}}^-)|$. Since $g_1(I_{\text{in}}) = g_2(I_{\text{in}})$, it follows that $g_1(x) > g_2(x)$ for x near I_{in}. By the intermediate value theorem, there exists a point $\hat{x} \in (0, I_{\text{in}})$ such that $g_1(\hat{x}) = g_2(\hat{x})$.

From $g_1(\hat{x}) = g_2(\hat{x})$, $g_1(I_{\text{in}}) = g_2(I_{\text{in}})$, there exists a point $\bar{x} \in (\hat{x}, I_{\text{in}})$ such that $g_1'(\bar{x}) = g_2'(\bar{x})$ according to Rolle's theorem. From (12) and (13), we have $p'(\bar{x}) = 0$. From assumption of $p(x)$, it follows that $\bar{x} = I_{\text{opt}}$. Hence, $\hat{x} < I_{\text{opt}} < I_{\text{in}}$.

Suppose there exists another point $\hat{x}' \in (0, I_{\text{in}})$ with $g_1(\hat{x}') = g_2(\hat{x}')$. If $\hat{x}' \in (\hat{x}, I_{\text{opt}}]$, then by Rolle's theorem there exists a point $s \in (\hat{x}, \hat{x}')$ such that $p'(s) = 0$. It contradicts to that $p'(I) > 0$ for $0 \leq I < I_{\text{opt}}$. If $\hat{x}' \in (I_{\text{opt}}, I_{\text{in}})$, then by Rolle's theorem there exists a point $s \in (I_{\mathrm{opt}}, I_{\mathrm{in}})$ such that $p'(s) = 0$. It contradict to that $p'(I) < 0$ for $0 \le I_{\mathrm{opt}} < I < I_{\mathrm{in}}$. Thus, $\hat{x}$ is the only point with $g_1(\hat{x}) = g_2(\hat{x})$.

Next, we prove the following theorem. In the following, we let $L(t) = I_{\mathrm{out}}(t)$ for convenience. From (11),

$$L(t) = I_0 \exp\left(-\sum_{j=1}^{n} k_j x_j(t)\right). \tag{14}$$

Theorem 2 *The solutions of* (10) *are positive and bounded.*

Proof Assume there exists $t_1 > 0$ and some $i \in \{1, 2, \ldots, n\}$ such that

$$\begin{aligned} &x_i(t_1) = 0, \qquad x_i(t) > 0 \quad \text{for } t \in [0, t_1), \\ &x_j(t) > 0 \quad \text{for } t \in [0, t_1] \text{ if } j \ne i. \end{aligned}$$

By reversing time, let $\tau = -t$ and we consider backward behavior of the solution of (10) with initial data $x_i(0) = 0, x_j(0) = x_j(t_1) > 0$. It follows that $x_i(\tau) = 0$ for all $\tau < 0$. By the uniqueness of ordinary differential equations, we have $x_i(-t_1) = 0$, a contradiction. Thus, the solutions are positive if the initial condition is in Ω.

To prove the boundedness of solution, we consider the differential inequalities

$$\begin{aligned} &x_i' = \bigl[g_i(L) - d_i\bigr]x_i \le \bigl[G_i(L) - d_i\bigr]x_i \le \bigl[G_i\bigl(I_0 \exp(-k_i x_i)\bigr) - d_i\bigr]x_i, \\ &\quad i = 1, 2, \ldots, n, \end{aligned}$$

where

$$G_i(s) = \begin{cases} g_i(s), & \text{for } 0 \le s \le L_{\max,i}, \\ \max_{s \in [0, I_0]} g_i(s), & \text{for } s \ge L_{\max,i} \end{cases}$$

with $g_i(L_{\max,i}) = \max_{s \in [0, I_0]} g_i(s)$. Let $y(t)$ be the solution of

$$y' = \bigl[G_i\bigl(I_0 \exp(-k_i y)\bigr) - d_i\bigr]y.$$

Then $\lim_{t\to\infty} y(t) = y_i$, where y_i satisfies $G_i(I_0 \exp(-k_i y_i)) - d_i = 0$. Hence, for given small ϵ, $x_i(t) \le y_i + \epsilon$ for all t large. Hence, $x_i(t)$ is bounded for all time t for $i = 1, 2, \ldots, n$. □

The next theorem says that if the light intensity is weak enough, then some species die out.

Theorem 3 *If* $\lambda_i > I_0$, *then* $\lim_{t\to\infty} x_i(t) = 0$.

Proof Since $L(t) \le I_0$ for all $t \ge 0$, we have $L(t) < \lambda_i$ for all $t \ge 0$. From $g_i(L(t)) \le G_i(L(t))$,

$$\frac{x_i'}{x_i} = g_i\bigl(L(t)\bigr) - d_i \le G_i\bigl(L(t)\bigr) - d_i \le G_i(I_0) - d_i < 0,$$

then $x_i(t) \to 0$ as $t \to \infty$. □

A.2 Local Stability of Equilibria

For simplicity, let

$$f_i\bigl(x_1(t), x_2(t), \dots, x_n(t)\bigr) := \bigl[g_i\bigl(L(t)\bigr) - d_i\bigr]x_i(t).$$

We denote the Jacobian of (10) at an equilibrium E is $J(E) = [m_{ij}] \in \mathbb{R}^{n\times n}$, where

$$\begin{aligned} m_{ii} &= \frac{\partial f_i}{\partial x_i} = \bigl[g_i(L) - d_i\bigr] - k_i g_i'(L)Lx_i, \\ m_{ij} &= \frac{\partial f_i}{\partial x_j} = -k_j g_i'(L)Lx_i, \quad \text{for } j \neq i. \end{aligned}$$

For the equilibrium E_0, the Jacobian at E_0 is

$$J(E_0) = \begin{bmatrix} g_1(I_0) - d_1 & 0 & 0 & \dots & 0 \\ 0 & g_2(I_0) - d_2 & 0 & \dots & 0 \\ \vdots & & & & \\ 0 & 0 & \dots & 0 & g_n(I_0) - d_n \end{bmatrix}.$$

Obviously the eigenvalues of $J(E_0)$ are $g_i(I_0) - d_i$, for $i = 1, 2, \dots, n$.

If $I_0 \notin S$, then $g_i(I_0) - d_i < 0$ for all i and E_0 is locally asymptotically stable.

If $I_0 \in S$, then there exists some i such that $I_0 \in (\lambda_i, \mu_i)$. Hence, $g_i(I_0) - d_i > 0$, and E_0 is unstable. If there exists some j such that $I_0 \notin (\lambda_j, \mu_j)$, then $J(E_0)$ has negative eigenvalues and E_0 is saddle with the local stable manifold

$$W^s_{\text{loc}}(E_0) = \left\{\sum_{i=1}^{n} c_i e_i : c_i = 0 \text{ except some } j \text{ with } I_0 \notin (\lambda_j, \mu_j).\right\},$$

where e_i is the eigenvector corresponding to the eigenvalue of $(g_i(I_0) - d_i)$. Hence, the dimension of $W^s(E_0)$, the stable manifold of E_0, is at most $(n-1)$ and

$$W^s(E_0) \subset \bigl\{(x_1, \dots, x_n) : x_i = 0 \text{ if } I_0 \in (\lambda_i, \mu_i)\bigr\}.$$

Therefore, $W^s(E_0) \cap \Omega = \emptyset$.

For the equilibria E_{λ_r}, the Jacobian evaluated at E_{λ_r} is

$$J(E_{\lambda_r}) = \begin{bmatrix} m_{11} & 0 & \dots & \dots & \dots & \dots & \dots & \dots & 0 \\ 0 & m_{22} & 0 & \dots & \dots & \dots & \dots & \dots & 0 \\ \vdots & & & & & & & & \\ 0 & \dots & 0 & m_{r-1,r-1} & 0 & \dots & \dots & \dots & 0 \\ m_{r1} & \dots & \dots & m_{r,r-1} & m_{r,r} & m_{r,r+1} & \dots & \dots & m_{rn} \\ 0 & \dots & \dots & \dots & 0 & m_{r+1,r+1} & 0 & \dots & 0 \\ \vdots & & & & & & & & \\ 0 & \dots & \dots & \dots & \dots & \dots & \dots & 0 & m_{nn} \end{bmatrix},$$

where

$$m_{jj} = g_j(\lambda_r) - d_j, \quad \text{for } j = 1, 2, \dots, r-1, r+1, \dots, n,$$
$$m_{ri} = -k_i x_{\lambda_r} g_r'(\lambda_r)\lambda_r, \quad \text{for } i = 1, 2, \dots, n.$$

The eigenvalues of $J(E_{\lambda_r})$ are $-k_r x_{\lambda_r} g_r'(\lambda_r)\lambda_r < 0$, and $g_j(\lambda_r) - d_j$, for all $j \neq r$.

When λ_r is the endpoint of a component of S, we have that $g_j(\lambda_r) - d_j < 0$ for $j \neq r$. Hence, E_{λ_r} is locally asymptotically stable.

If λ_r is not the endpoint of a component of S, then there exists j such that $\lambda_r \in (\lambda_j, \mu_j)$. The eigenvector corresponding to the negative eigenvalue $-k_r x_{\lambda_r} g_r'(\lambda_r)\lambda_r$ is

$$v_r = (0, \dots, 0, x_r, 0, \dots, 0), \quad x_r > 0 \text{ in the } r\text{th component},$$

and the eigenvectors corresponding to the negative eigenvalues $g_i(\lambda_r) - d_i$ are

$$v_i = (0, \dots, 0, k_r, 0, \dots, 0, -k_i, 0, \dots, 0),$$

where $k_r,\ k_j > 0$ are in the ith , and rth component of vector v_i, respectively. We know that E_{λ_r} is saddle and the local stable manifold is

$$W^s_{\mathrm{loc}}(E_{\lambda_r}) = \left\{ E_{\lambda_r} + \sum_{i=1}^{n} c_i v_i :\ c_i = 0 \text{ except } c_r \text{ and some } j \text{ with } \lambda_r \notin (\lambda_j, \mu_j) \right\}.$$

Hence, the stable manifold of E_{λ_r} is

$$W^s(E_{\lambda_r}) \subset \big\{ (x_1, \dots, x_n) : x_i = 0 \text{ if } \lambda_r \in (\lambda_i, \mu_i) \big\},$$

and $W^s(E_{\lambda_r}) \cap \Omega = \emptyset$.

For the equilibria E_{μ_r}, the Jacobian evaluated at E_{μ_r} is $J(E_{\mu_r})$, the structure is similar to $J(E_{\lambda_r})$ and

$$m_{jj} = g_j(\mu_r) - d_j, \quad \text{for } j = 1, 2, \dots, r-1, r+1, \dots, n,$$
$$m_{ri} = -k_i x_{\mu_r} g_r'(\mu_r)\mu_r, \quad \text{for } i = 1, 2, \dots, n.$$

The eigenvalues are $-k_r x_{\mu_r} g_r'(\mu_r)\mu_r > 0$, an $g_j(\mu_r) - d_j$, for all $j \neq r$.

For the case μ_r is the endpoint of a component of S, then $g_j(\mu_r) - d_j < 0$ for all $j \neq r$. Hence, E_{μ_r} is saddle with one dimensional unstable manifold

$$W^u(E_{\mu_r}) = \big\{ E_{\mu_r} + s v_r : v_r = (0, \dots, 0, x_r, 0, \dots, 0), x_r > 0 \text{ in the } r\text{th component} \big\}.$$

The eigenvectors corresponding to the negative eigenvalues $g_j(\lambda_r) - d_j$ for all $j \neq r$ are

$$v_j = (0, \dots, 0, k_r, 0, \dots, 0, -k_j, 0, \dots, 0),$$

where $k_r,\ k_j > 0$ are in the jth, and rth components of the vector v_j, respectively. E_{μ_r} is saddle which stable manifold $W^s(E_{\mu_r})$ is tangent to

$$W^s_{\mathrm{loc}}(E_{\mu_r}) = \left\{ E_{\mu_r} + \sum_{j=1}^{n} c_j v_j : c_r = 0, c_j \neq 0, \text{ for } j \neq r \right\},$$

at E_{μ_r}. Thus, the $(n-1)$-dimensional stable manifold of E_{μ_r} satisfies

$$W^s(E_{\mu_r}) \subset \{(x_1, x_2, \ldots, x_n), x_i > 0 \text{ for all } i\},$$

and $W^s(E_{\mu_r}) \cap \Omega \neq \emptyset$.

For the case μ_r is not the endpoint of a component of S, then there exists j such that $\mu_r \in (\lambda_j, \mu_j)$ and $g_j(\lambda_r) - d_j > 0$. If there exists some i such that $\mu_r \in (\lambda_i, \mu_i)$, then E_{μ_r} is saddle which stable manifold $W^s(E_{\mu_r})$ is tangent to

$$W^s_{\text{loc}}(E_{\mu_r}) = \left\{ E_{\mu_r} + \sum_{j=1}^{n} c_j v_j : c_j = 0 \text{ except } c_i \text{ with } \mu_r \notin (\lambda_i, \mu_i) \right\},$$

at E_{μ_r}. Hence, the stable manifold of E_{μ_r} is

$$W^s(E_{\mu_r}) \subset \{(x_1, \ldots, x_n) : x_i = 0 \text{ if } \mu_r \in (\lambda_i, \mu_i)\},$$

and $W^s(E_{\mu_r}) \cap \Omega = \emptyset$.

A.3 The Proof of Theorem 1

To prove Theorem 1, we need the following three lemmas. We note that the following proofs are similar to those in Butler and Wolkowicz (1985). We present them for the sake of completeness of the paper.

Lemma 4 *If* $\lim_{t\to\infty} x_i(t) > 0$, *then* $\lim_{t\to\infty} L(t) = \lambda_i$ *or* μ_i *and* $\lim_{t\to\infty} x_j(t) = 0$ *for* $j \neq i$.

Proof Since $\lim_{t\to\infty} x_i(t)$ exists and it is positive, and $|x_i''(t)|$ is bounded, then $x_i'(t)$ converges to 0 as t goes to infinity, i.e.,

$$g_i\bigl(L(t)\bigr) - d_i \to 0 \quad \text{as } t \to \infty.$$

Therefore, $\lim_{t\to\infty} L(t) = \lambda_i$ or μ_i.

For $j \neq i$, we prove $\lim_{t\to\infty} x_j(t) = 0$ by contradiction. First, we assume $\lim_{t\to\infty} x_j(t) > 0$, then by the similar argument as above, we obtain that $\lim_{t\to\infty} L(t) = \lambda_j$ or μ_j, a contradiction. Thus, $\lim_{t\to\infty} x_j(t)$ does not exist and $\limsup_{t\to\infty} x_j(t) > 0$. Then there exists a subsequence t_m increases to infinity as m goes to infinity, and $x_j(t_m)$ converges to $\limsup_{t\to\infty} x_j(t)$ and $x_j'(t_m) = 0$. Hence, $g_j(L(t_m)) - d_j = 0$ and $L(t_m) = \lambda_j$ or μ_j, a contradiction to $\lim_{t\to\infty} L(t) = \lambda_i$ or μ_i. Thus, we have $\lim_{t\to\infty} x_j(t) = 0$. □

Lemma 5 *If* $\lim_{t\to\infty} L(t) = \gamma$, *then* $\gamma \in \{I_0,$ *the endpoints of a component of* $S\}$.

1. *If* $\gamma = I_0$, *then* $I_0 \notin S$, *and* $\lim_{t\to\infty} x_i(t) = 0$ *for all* i.
2. *If* $\gamma = \lambda_i$ *or* μ_i, *the endpoint of a component of* S, *then* $\gamma < I_0$ *and* $\lim_{t\to\infty} x_i(t) = x_{\lambda_i}$ *or* x_{μ_i} *and* $\lim_{t\to\infty} x_j(t) = 0$ *for* $j \neq i$.

Proof We prove by contradiction. If not, then $\gamma \notin \{I_0,$ the endpoints of a component of $S\}$. There are two possibilities: $\gamma \in S$ and $\gamma \notin S$.

If $\gamma \in S$, from the assumption $\lim_{t\to\infty} L(t) = \gamma$, then for $\epsilon > 0$ there exists some i and $T_\epsilon > 0$ such that $L(t) \subset (\lambda_i, \mu_i)$ for $t \geq T_\epsilon$. It follows that $x_i'(t) \geq 0$ for $t \geq T_\epsilon$, and from the fact $x_i(t)$ is bounded above, then $\lim_{t\to\infty} x_i(t) > 0$. By Lemma 4, we have that $\gamma = \lim_{t\to\infty} L(t) = \lambda_i$ or μ_i. Since γ is not endpoints of S, there exists $j \neq i$ such that $\gamma \in (\lambda_j, \mu_j)$. It follows that $L(t) \subset (\lambda_j, \mu_j)$ for all large t. By similar argument as above, we have $\lim_{t\to\infty} L(t) = \lambda_j$ or μ_j, a contradiction.

If $\gamma \notin S$, then for $\epsilon > 0$ there exists $T_\epsilon > 0$ s.t. $L(t) \in (\gamma - \epsilon, \gamma + \epsilon) \subset S^c$ for $t \geq T_\epsilon$. Hence $\frac{x_i'(t)}{x_i(t)} = g_i(L(t)) - d_i < 0$ for all i for $t \geq T_\epsilon$. Therefore, $\lim_{t\to\infty} x_i(t) = 0$ for all i, and $\lim_{t\to\infty} L(t) = I_0$, a contradiction.

1. Let $\gamma = I_0$. Assume $I_0 \in S$ and from the convergence of $L(t)$, there exists i such that $L(t) \in (\lambda_i, \mu_i)$ for all t is large. By similar argument as above, we have $\lim_{t\to\infty} x_i(t) > 0$ and $\lim_{t\to\infty} L(t) = \lambda_i$ or μ_i, it is a contradiction. Thus, $I_0 \notin S$.

   Now we prove $\lim_{t\to\infty} x_i(t) = 0$ for all i by contradiction. First we assume that there exists i such that $\lim_{t\to\infty} x_i(t) > 0$. Then $\lim_{t\to\infty} L(t) = \lambda_i$ or μ_i, a contradiction. Assume $\lim_{t\to\infty} x_i(t)$ does not exist and $\limsup_{t\to\infty} x_i(t) > 0$. Then there exists a sequence $\{t_m\}$ increases to infinity as t goes to infinity such that $x_i'(t_m) = 0$ and $\lim_{m\to\infty} x_i(t_m) = \limsup_{t\to\infty} x_i(t)$. It follows that $g_i(L(t_m)) - d_i = 0$ and $L(t_m) = \lambda_i$ or μ_i for all m, a contradiction to $\gamma = I_0$. Thus, $\lim_{t\to\infty} x_i(t) = 0$ for all i.
2. It is clear that $\gamma < I_0$, since $L(t) \leq I_0$ for all t. $\lim_{t\to\infty} x_j(t) = 0$ for $j \neq i$ follows from the above argument. Thus, it follows that $\lim_{t\to\infty} L(t) = \lim_{t\to\infty}[I_0 e^{-k_i x_i(t)}] = \lambda_i$ or μ_i, or equivalently $\lim_{t\to\infty} x_i(t) = x_{\lambda_i}$ or x_{μ_i}. □

Lemma 6 *$L(t)$ converges as t goes to infinity.*

Proof If not, then there exist increasing sequences $\{t_m\}$, $\{\tau_m\}$ such that

$$L'(t_m) = 0, \lim_{m\to\infty} L(t_m) = \limsup_{t\to\infty} L(t) := \overline{L},$$

$$L'(\tau_m) = 0, \lim_{m\to\infty} L(\tau_m) = \liminf_{t\to\infty} L(t) := \underline{L}.$$

Note that there are some $i \in \{1, 2, \ldots, n\}$ such that $x_i(t)$ do not tend to zero. Since

$$L'(t_m) = -L(t_m)\left[\sum_{i=1}^{n} k_i x_i'(t_m)\right] = 0,$$

for each m there are some $j_m \in \{1, 2, \ldots, n\}$ satisfies $x_{j_m}'(t_m) \geq 0$. There exists some j such that $j_m = j$ for infinitely many m. For this j, we choose a subsequence of $\{t_m\}$, also named $\{t_m\}$, such that $x_j'(t_m) \geq 0$. It follows that $L(t_m) \in [\lambda_j, \mu_j]$ for all m and $\overline{L} \in [\lambda_j, \mu_j]$. Similarly, we can find some k and a subsequence of $\{\tau_m\}$, also named $\{\tau_m\}$, such that $L(\tau_m) \in [\lambda_k, \mu_k]$ for all m and $\underline{L} \in [\lambda_k, \mu_k]$.

If $\overline{L} \in [\lambda_j, \mu_j] \subset [\lambda_{p_1}, \mu_{q_1}]$ and $\underline{L} \in [\lambda_k, \mu_k] \subset [\lambda_{p_2}, \mu_{q_2}]$ where $(\lambda_{p_1}, \mu_{q_1})$ and $(\lambda_{p_2}, \mu_{q_2})$ are two disjoint components of S. Then there exists an increasing sequence

$\{s_m\}$ with $t_m < s_m < \tau_m$ such that $L'(s_m) < 0$ and $L(s_m) \in (\mu_{q_2}, \lambda_{p_1}) \cap S^c$ for all m. Hence, $x_i'(s_m) < 0$ for all i and $L'(s_m) > 0$, a contradiction.

Thus, $[\lambda_j, \mu_j]$ and $[\lambda_k, \mu_k]$ belong to the same set $[\lambda_p, \mu_q]$, that is, $\overline{L}$ and $\underline{L}$ belong to $[\lambda_p, \mu_q]$, where (λ_p, μ_q) is a component of S.

If there does not exist $\gamma \in \Gamma$, $\Gamma = \{\lambda_i,\ \mu_i : i = 1, 2, \dots, n\}$, s.t. $\gamma \in (\underline{L}, \overline{L})$, then there exists some r s.t. $L(t) \in [\lambda_r, \mu_r] \subset [\lambda_p, \mu_q]$ for all large t. Then we have $x_r'(t) > 0$ for all large t. From the boundedness of x_r, it follows that $\lim_{t\to\infty} x_r(t) = x_r^* \geq 0$ and $\lim_{t\to\infty} L(t) = \lambda_r$ or μ_r, a contradiction.

Thus, there exists some $\gamma \in \Gamma$ s.t. $\gamma \in (\underline{L}, \overline{L})$, let $\gamma_1,\ \gamma_2$ be two consecutive elements of Γ such that $\gamma_1 < \underline{L} < \gamma_2$. Since $L(t)$ oscillates, there exists $T_1 < T_2$ such that $L(T_1) = L(T_2) = \gamma_2,\ \gamma_1 < L(t) \leq \gamma_2$ for $t \in [T_1, T_2]$ and $L'(T_1) < 0 < L'(T_2)$. From

$$L'(t) = -L(t)\left[\sum_{i=1}^{n} k_i x_i'(t)\right],$$

we have

$$\sum_{i=1}^{n} k_i x_i'(T_1) > 0 > \sum_{i=1}^{n} k_i x_i'(T_2).$$

We divide the above summation into two parts, one is $x_i'(T_j) < 0$, i.e. $g_i(\gamma_2) < d_i$, the other is $x_i'(T_j) > 0$, i.e. $g_i(\gamma_2) > d_i$. Therefore, we have

$$\sum_{g_i(\gamma_2)<d_i} k_i x_i'(T_1) + \sum_{g_i(\gamma_2)>d_i} k_i x_i'(T_1) > \sum_{g_i(\gamma_2)<d_i} k_i x_i'(T_2) + \sum_{g_i(\gamma_2)>d_i} k_i x_i'(T_2),$$

and

$$\begin{aligned} &-\sum_{g_i(\gamma_2)<d_i} k_i\big[g_i(\gamma_2) - d_i\big]\big(x_i(T_2) - x_i(T_1)\big) \\ &\quad > \sum_{g_i(\gamma_2)>d_i} k_i\big[g_i(\gamma_2) - d_i\big]\big(x_i(T_2) - x_i(T_1)\big). \end{aligned} \tag{15}$$

For the case $g_i(\gamma_2) < d_i$, i.e., $\gamma_2 \notin (\lambda_i, \mu_i)$, then $L([T_1, T_2])$ is disjoint from (λ_i, μ_i). Hence, $x_i'(t) < 0$ for $t \in [T_1, T_2]$ and $x_i(T_2) < x_i(T_1)$. For the case $g_i(\gamma_2) > d_i$, i.e., $\lambda_i < \gamma_2 < \mu_i$, we have $L([T_1, T_2]) \subset (\lambda_i, \mu_i)$. Hence $x_i'(t) > 0$ for $t \in [T_1, T_2]$ and $x_i(T_2) > x_i(T_1)$. Thus,

$$\begin{aligned} &-\sum_{g_i(\gamma_2)<d_i} k_i\big[g_i(\gamma_2) - d_i\big]\big(x_i(T_2) - x_i(T_1)\big) < 0 \\ &\quad < \sum_{g_i(\gamma_2)>d_i} k_i\big[g_i(\gamma_2) - d_i\big]\big(x_i(T_2) - x_i(T_1)\big), \end{aligned}$$

a contradiction to (15). Hence, the theorem holds. □

References

Alderkamp, A. C., de Baar, H. J. W., Visser, R. J. W., & Arrigo, K. R. (2010). Can photoinhibition control phytoplankton abundance in deeply mixed water columns of the Southern Ocean? *Limnol. Oceanogr.*, *55*, 1248–1264.

Andrews, J. F. (1968). A mathematical model for the continuous culture of microorganisms utilizing inhibitory substrates. *Biotechnol. Bioeng.*, *10*, 707–723.

Baastrup-Spohr, L., & Staehr, P. A. (2009). Surface microlayers on temperate lowland lakes. *Hydrobiologia*, *625*, 43–59.

Basterretxea, G., & Aristegui, J. (2000). Mesoscale variability in phytoplankton biomass distribution and photosynthetic parameters in the Canary–NW African coastal transition zone. *Mar. Ecol. Prog. Ser.*, *197*, 27–40.

Bischof, K., Hanelt, D., & Wiencke, C. (1998). UV-radiation can affect depth-zonation of Antarctic macroalgae. *Mar. Biol.*, *131*, 597–605.

Bouchard, J. N., Roy, S., & Campbell, D. A. (2006). UVB effects on the photosystem II-D1 protein of phytoplankton and natural phytoplankton communities. *Photochem. Photobiol.*, *82*, 936–951.

Butler, G. J., & Wolkowicz, G. S. K. (1985). A mathematical model of the chemostat with a general class of functions describing nutrient uptake. *SIAM J. Appl. Math.*, *45*, 138–151.

Eilers, P. H. C., & Peeters, J. C. H. (1988). A model for the relationship between light intensity and the rate of photosynthesis in phytoplankton. *Ecol. Model.*, *42*, 199–215.

Elser, J. J., & Kimmel, B. L. (1985). Photoinhibition of temperate lake phytoplankton by near-surface irradiance: evidence from vertical profiles and field experiments. *Eur. J. Phycol.*, *21*, 419–427.

Gerla, D. J., Mooij, W. M., & Huisman, J. (2011). Photoinhibition and the assembly of light-limited phytoplankton communities. *Oikos*, *120*, 359–368.

Han, B. P. (2002). A mechanistic model of algal photoinhibition induced by photodamage to photosystem-II. *J. Theor. Biol.*, *214*, 519–527.

Henley, W. J. (1993). Measurement and interpretation of photosynthetic light-response curves in algae in the context of photoinhibition and diel changes. *Eur. J. Phycol.*, *29*, 729–739.

Huisman, J. (1997). *The struggle for light*. Ph.D. thesis, Rijksuniversiteit Groningen.

Huisman, J., & Weissing, F. J. (1994). Light-limited growth and competition for light in well-mixed aquatic environments: an elementary model. *Ecology*, *75*, 507–520.

Huisman, J., & Weissing, F. J. (1995). Competition for nutrients and light in a mixed water column: a theoretical analysis. *Am. Nat.*, *146*, 536–564.

Klausmeier, C. A., & Litchman, E. (2001). Algal games: the vertical distribution of phytoplankton in poorly mixed water columns. *Limnol. Oceanogr.*, *46*, 1998–2007.

Kohyama, T. (1993). Size-structured tree populations in gap-dynamic forest: the forest architecture hypothesis for the stable coexistence of species. *J. Ecol.*, *81*, 131–143.

Litchman, E., & Klausmeier, C. A. (2008). Trait-based community ecology of phytoplankton. *Annu. Rev. Ecol. Evol. Syst.*, *39*, 615–639.

Litchman, E., & Neale, P. J. (2005). UV effects on photosynthesis, growth and acclimation of an estuarine diatom and cryptomonad. *Mar. Ecol. Prog. Ser.*, *300*, 53–62.

Litchman, E., Neale, P. J., & Banaszak, A. T. (2002). Increased sensitivity to ultraviolet radiation in nitrogen-limited dinoflagellates: photoprotection and repair. *Limnol. Oceanogr.*, *47*, 86–94.

McGill, B. J., Enquist, B. J., Weiher, E., & Westoby, M. (2006). Rebuilding community ecology from functional traits. *Trends Ecol. Evol.*, *21*, 178–185.

Mellard, J. P., Yoshiyama, K., Litchman, E., & Klausmeier, C. A. (2011). The vertical distribution of phytoplankton in stratified water columns. *J. Theor. Biol.*, *269*, 16–30.

Muller, E. B. (2010). Synthesizing units as modeling tool for photosynthesizing organisms with photoinhibition and nutrient limitation. *Ecol. Model.*, *222*, 637–644.

Oliver, R. L., Whittington, J., Lorenz, Z., & Webster, I. T. (2003). The influence of vertical mixing on the photoinhibition of variable chlorophyll *a* fluorescence and its inclusion in a model of phytoplankton photosynthesis. *J. Plankton Res.*, *25*, 1107–1129.

Ryabov, A. B., Rudolf, L., & Blasius, B. (2010). Vertical distribution and composition of phytoplankton under the influence of an upper mixed layer. *J. Theor. Biol.*, *263*, 120–133.

Schwaderer, A. S., Yoshiyama, K., de Tezanos Pinto, P., Swenson, N. G., Klausmeier, C. A., & Litchman, E. (2011). Eco-evolutionary differences in light utilization traits and distributions of freshwater phytoplankton. *Limnol. Oceanogr.*, *56*, 589–598.

Stomp, M., Huisman, J., Voros, L., Pick, F. R., Laamanen, M., Haverkamp, T., & Stal, L. J. (2007). Colourful coexistence of red and green picocyanobacteria in lakes and seas. *Ecol. Lett.*, *10*, 290–298.

Tyystjärvi, E. (2008). Photoinhibition of photosystem II and photodamage of the oxygen evolving manganese cluster. *Coord. Chem. Rev.*, *252*, 361–376.

Weissing, F. J., & Huisman, J. (1994). Growth and competition in a light gradient. *J. Theor. Biol.*, *168*, 323–336.

Yoshiyama, K., Mellard, J. P., Litchman, E., & Klausmeier, C. A. (2009). Phytoplankton competition for nutrients and light in a stratified water column. *Am. Nat.*, *174*, 190–203.

Yoshiyama, K., & Nakajima, H. (2002). Catastrophic transition in vertical distributions of phytoplankton: alternative equilibria in a water column. *J. Theor. Biol.*, *216*, 397–408.

Zonneveld, C. (1998). Photoinhibition as affected by photoacclimation in phytoplankton: a model approach. *J. Theor. Biol.*, *193*, 115–123.